Spatial and temporal dynamics of cropland in the Sanjiang Plain from 2014 to 2020 based on annual 30 m crop data layers

Cui Jin[1] ⓘ, Zeyu Zhang[1], Hongyan Cai[2], Ge Cao[1], Xintao Li[3] and Xueming Li[1]

[1]School of Geography, Liaoning Normal University, 850 Huanghe Road, Dalian 116029, China; [2]State Key Laboratory of Resources and Environmental Information Systems, Institute of Geographic Sciences and Natural Resources Research, Chinese Academy of Sciences, 11A Datun Road, Beijing 100101, China and [3]School of Earth Sciences and Engineering, Hohai University, Nanjing 210098, China

Abstract

The land cover of the Sanjiang Plain has changed dramatically since the 1950s. Although previous studies have analysed its spatiotemporal dynamics at long time intervals, a near real-time and accurate representation of the interannual evolution of cropping patterns in this region is of far-reaching importance for rationally allocating agricultural resources and ensuring food security. Based on the 30 m and 10 m land cover datasets in 2015 and 2017–2019, the current study used Landsat-8 satellite data in 2014, 2016 and 2020 to identify paddy rice and dryland crops using a decision tree classification approach and constructed the annual cropland datasets of the Sanjiang Plain from 2014 to 2020. The results show that the overall classification accuracies of crop datasets exceeded 95%, and the Kappa coefficients were higher than 0.92. The average annual accuracies of users and producers were 93% and 94% for rice fields and 97% and 95% for dryland crops, respectively. During the 7 years, the total area of paddy fields and dryland crops decreased by 5% and 8%. However, with minor positive and negative variation between years. 24.2% of paddy rice and 42% of dryland crops has been cultivated under 4 years. The centres of gravity for both crops mainly aggregated in the central counties with the migration direction and magnitude varying interannually. The current study emphasizes the importance of establishing annual high-resolution crop datasets to track the detailed spatio-temporal trajectories of cropping patterns that are essential to support sustainable cropland management and agricultural development.

Introduction

The Sanjiang Plain is one of the most important commodity grain bases in China (Shi *et al.*, 2020). The large-scale land reclamations in this region have mainly happened before 21st century; However, the cropping structures have still undergone significant changes every year recently due to the government's crop rotation project (Cai *et al.*, 2021) and soybean rejuvenation programme (e.g. rice-to-soybean conversion) (Lin, 2023). Quantitative information about present interannual cropping structure changes is still limited. Despite some efforts in short-period annual crop mapping (You *et al.*, 2021), yearly-temporal and fine-spatial crop type maps during recent periods of dramatic planting structure alterations remain absent. Thus, it limits our understanding the ongoing process of farm trajectories and its related driving factors behind these dynamics in this region.

Remote sensing technology can provide information on cropping structure and its dynamics at regional and global scales (Zhang *et al.*, 2021). Satellite data with low spatial (250 m–1 km) and high temporal (daily to monthly) resolution (i.e., MODIS and AVHRR) have been widely used for large-scale extraction of crop types (Wardlow *et al.*, 2007; Chen *et al.*, 2018). However, for smallholder farming, areas or regions with diverse cultivation structures or complex terrain regions, the 'mixed pixel' problems in satellite data with coarse spatial resolution lead to significant errors in crop mapping and even in production estimation due to heterogeneous agricultural landscapes (Hu *et al.*, 2021; Luo *et al.*, 2022). Public Free and open access to long time series of remote sensing data with medium to high spatial and temporal resolution offers new opportunities for large-scale crop mapping; Meanwhile, standardized and operational crop-classification platforms have been well established (Song *et al.*, 2021). In particular, the dense time series of Landsat and Sentinel data (10-30 m) limit the mixed-pixel problems, and have been applied to map the precise annual spatial distribution of crops at the national and continental scales. For instance, the U.S. Department of Agriculture's (USDA) Cropland Data Layers (CDLs) are 30 m satellite imagery-derived crop-specific land cover maps across the conterminous United States. The CDLs are produced using multi-source satellite imagery (i.e., Landsat, Resourcesat, Sentinel, etc.), and have been

CAMBRIDGE UNIVERSITY PRESS

annually updated since 2008. The CDLs include 110 land and crop classes with an average classification accuracy of over 90% (Boryan et al., 2011). The Agriculture and Agri-Food Canada (AAFC) has generated the annual crop type digital maps in Canada since 2009, a decision tree based methodology was applied using optical (Landsat-5, AWiFS, DMC) and radar (Radarsat-2) based satellite images, and the overall accuracy is at least 85% (Fisette et al., 2013; Amani et al., 2020). Blickensdörfer et al. (2022) combined the time series of Sentinel-1, Sentinel-2 and Landsat-8 data to map 24 agricultural land cover classes in Germany for the 3 consecutive years (2017, 2018 and 2019). For cross-national scales, under the support of the European Space Agency (ESA), the Sen2-Agri system allows for automated agricultural land cover maps derived from Sentinel-2 and Landsat-8 imagery at 10 m spatial resolution (Defourny et al., 2019). In addition, Luo et al. (2022) applied transductive transfer learning to process 130 000 Sentinel-2 images on the Google Earth Engine (GEE) platform, and generated the 10 m crop maps for four major crops across 10 European Union (EU) countries for 2018 and 2019. So far, systematic technical classification systems and platforms based on remote sensing data with medium and high spatial resolution have been established in Europe and America for regional crop mapping. These continuously improve the generation of annual crop data, which provide the necessary research basis for analysing the evolution of cropping structure at multi-spatial and temporal scales. However, in China, systematic, automated and wall-to-wall monitoring of the cropland mapping system has received less attention (You et al., 2021); and current available high-resolution cropland data not only cover a limited number of crop types, but are also irregularly updated.

The Sanjiang Plain has experienced intensive land reclamations since 1950s. Even though the dynamic evolution of land cover in the Sanjiang Plain has been well studied, the up-to-date crop dynamics is unknown due to the unavailability of fine-scale and annual continuous cropland maps. The current study summarized the literatures on the spatial and temporal dynamics of cropland in the Sanjiang Plain in terms of remote sensing data, classification methods and time spans and intervals (Table 1). As for the data, the studies used remote sensing data with medium spatial resolution such as Landsat as the main data source. In terms of classification methods, visual image interpretation (Song et al., 2008, 2017; Wang et al., 2009; Yan et al., 2016a, 2016b; Zhang et al., 2022), supervised classification (Pan et al., 2018), phenology-based methods (Dong et al., 2015) or object-oriented approaches (Xie et al., 2021) were used to map cropping patterns for individual years in the study area; For the study periods, the studies focused on the years before 2015; meanwhile, the time spans for quantifying the spatial and temporal dynamics of croplands were long (5–12 years). Crop cultivation in the Sanjiang Plain is intensive. Under the influence of temperature and precipitation, management policies, etc., annual fluctuation of crop planting structure is relatively significant. Therefore, it is urgent to establish high-resolution annual crop distribution datasets to update the continuous interannual cropland cultivation evolutions in the Sanjiang Plain in recent years. For this purpose, the specific objectives of the current study were to: (1) construct annual 30 m cropland data layers in the Sanjiang Plain from 2014 to 2020; (2) explore temporally high-frequency and spatially continuous dynamic change patterns of paddy rice and dryland crops.

Table 1. Studies related to time-series geospatial datasets for croplands in the Sanjiang Plain

Study area	Satellite data	Study years (Interval)	Classification method	Crop types	Reference
Sanjiang Plain	Landsat MSS/TM/ETM+CBERS-2	1954–2005 (>5)	Visual interpretation	Paddy rice, dryland crops, etc.	Song et al. (2008), Huang et al. (2009), Wang et al. (2009)
Sanjiang Plain	Landsat MSS/TM/ETM+/OLI	1990–2015 (5, 10, 14)	Visual interpretation	Paddy rice, dryland crops, etc.	Yan et al. (2016a, 2016b)
Qixinghe area	Landsat TM/OLI	1990–2014 (12)	Visual interpretation	Paddy rice, dryland crops, etc.	Song et al. (2017)
Sanjiang Plain	Landsat TM/OLI	2000–2015 (5)	Visual interpretation	Paddy rice, dryland crops	Zhang et al. (2022)
North region	Landsat TM/ETM CBERS-2	2000–2009 (10)	Human-computer interactive interpretation	Paddy rice, dryland crops	Du et al. (2012)
Northeast region	Landsat TM/ETM+	1986–2010 (5)	Phenology-based classification	Paddy rice	Dong et al. (2015)
North region	Landsat MSS/TM/ETM+/OLI	1975–2013 (>6)	Object-oriented classification	Crop land, etc.	Xie et al. (2021)
Sanjiang Plain	Landsat MSS/TM/ETM+/OLI	1990–2015 (5)	Supervised classification	Paddy rice, dryland crops	Pan et al. (2018), Pan et al. (2020), Pan et al. (2021)

Materials and methods

Study area

The Sanjiang Plain is located in northeastern Heilongjiang Province, China (43.834°N–48.411°N, 129.196°E–134.776°E) and covers a total area of 10.87×10^4 km² and 23 counties (Fig. 1). It is formed by the alluviation of Helongjiang, Songhuajiang and Wusulijiang rivers. The climate of this region varies between temperate humid and subhumid continental monsoon, with average temperatures below −18 °C in January and 21–22°C in July and average annual precipitation of 500–650 mm. The suitable climate, flat terrain, fertile soil and sufficient water resources offer the favourable optimal conditions for agricultural cultivation. Rice, maize and soybeans are the three major crops, which mainly distribute in the flatlands of the northeast, central and sourtheast Sanjiang Plain and present a mosaic spatial landscape (Yin et al., 2020). Paddy rice is irrigated, but other crops (such as corn and soybeans) are dryland crops (Fan et al., 2020). From 2003 to 2015, the total cultivation area of crops showed a fluctuating upward trend, and the total grain production increased continuously. In 2015, the sown area of three crops was about 96% of the Sanjiang Plain's total crop cultivation area, with corn accounting for 40%, rice 37% and soybeans 19% (Cai et al., 2021).

Data and preprocessing

The datasets for the current study include: (1) Landsat-8 surface reflectance data were collected from 2014–2021, with a spatial resolution of 30 m and a temporal resolution of 16 days (Table 2). The satellite data covered the period from rice field flooding to rice sowing (late April to June) with a total of 32 image scenes. When the cloud cover of the images in 2014, 2016 and 2020 was more than 5%, cloud-free images from the same period of adjacent years were selected for cloud-mask replacement. Since the Landsat-8 surface reflectance data have been radiometrically and atmospherically corrected, the image preprocessing in the current study included projection transformation, coordinate matching, clipping and image mosaicing; (2) The 2015 Northeast China Land Use Data (NCLUD2015) was derived from Landsat-8 imagery using an object-oriented classification approach. The NCLUD2015 croplands include two types (paddy rice and dryland crops) with an overall accuracy of 94% (Mao et al., 2018; Mao et al., 2019); (3) Then collected the 10 m crop data layer for northeast China (NCCDL10 m) developed by You et al. (2021). This dataset included 3 years of crop data layers during 2017–2019, which were produced using time-series Sentinel-2 imagery and random forest algorithm on the GEE platform. The dataset mapped 3 most popular crop types (corn, soybean and paddy rice) with an overall accuracy of 81%-86% over three years. To match with land use classification system of NCLUD2015, corn and soybean were combined as dryland crops. The NCLUD2015 and NCCDL10m datasets used different classification systems, which made the comparison difficult. The current work first aggregated these maps by reclassifying them using a unified legend system, which includes three land cover types: paddy rice, dryland crops and non-crop.
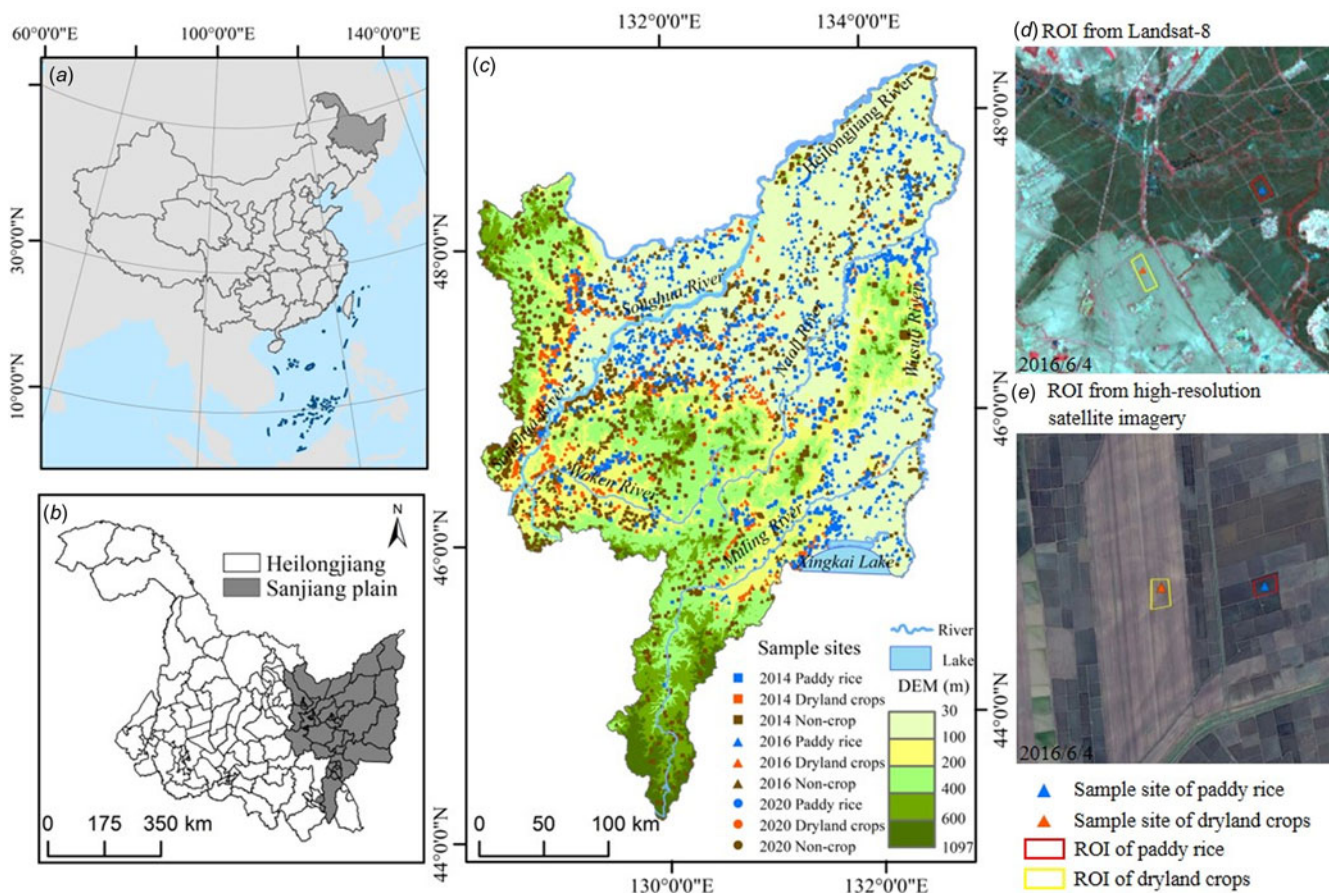

Fig. 1. Location of the Sanjiang Plain (a–b); Spatial distribution of validation sample sites in 2014/2016/2020 (c); Gound-reference ROI examples from Landsat-8 (d) and high-resolution images (e).

Table 2. Landsat-8 surface reflectance data

Year	Image time	Path/Row	Cloud fraction/%	Year	Image time	Path/Row	Cloud fraction/%
2014	2014-05-25	113/27	11.06	2016	2017-06-16	115/27	0.63
	2014-06-01	114/26	17.26		2017-06-16	115/29	3.51
	2014-05-30 △	116/28	15.44		2016-06-04	116/26	18.61
	2015-05-10 ▲	115/28	0.02		2016-06-04	116/27	1.33
	2014-06-01	114/28	0.93		2016-05-19	116/28	0.13
	2015-05-01	116/29	2.81		2016-05-19	116/29	0.01
	2015-05-10	115/26	0.34	2020	2020-06-10	113/27	4.02
	2015-05-10	115/27	0		2021-05-03	114/26	7.03
	2015-05-17	116/26	19.92		2021-05-03	114/27	5.33
	2015-06-01	114/27	2.67		2020-05-07	115/26	0.04
2016	2016-05-14	113/26	23.21		2020-05-07	115/27	0.02
	2017-05-01	113/27	22.43		2020-05-07	116/26	0.43
	2015-06-14	114/27	3.46		2020-05-07	116/27	0.01
	2016-05-21 △	114/28	8.65		2020-05-07 △	115/28	4.45
	2017-06-16 ▲	115/28	1.02		2021-05-17 ▲	116/28	0
	2016-05-21	114/29	0.01		2021-05-17	116/29	0.02

Note: △ Images with cloud cover > 5%, ▲ images for cloud-covered area replacement. Other unlabelled images with more than 5% clouds will only use the cloud-free part of the image in the mosaic and clip.

Classification and validation of paddy rice and dryland crops

To construct a 30-m annual-continuous crop dataset of the Sanjiang Plain during 2014–2020, the current study collected four years of currently available cropland spatial datasets in 2015 and 2017–2019; the current work proposed a two-step conceptual framework of decision tree classification to generate crop data layers for the other three years of 2014, 2016 and 2020, based on the above cropland datasets and Landsat-8 satellite data as follows (Fig. 2):

Step 1 to generate crop and non-crop layers: the current study used the Landsat-8 colour composite images in 2014, 2016 and 2020 as ground truth, and manually updated the crop and non-crop boundaries of neighbouring years of 2015, 2017 and 2019 by visual interpretation methods;

Step 2 to identify paddy rice and dryland crops within crop layers using the decision rule of the Modified Normalized Difference Water Index (MNDWI) at the pixel scale: the rice fields of the Sanjiang Plain are flooded between late April and early May, and rice seedling transplantation begins in mid-May. From late April to mid-June, the rice fields show mixed spectral features of water and seedlings on the Landsat-8 images. Meanwhile, the dryland crop fields show a mixed spectrum of dry-bare soil and seedlings. Therefore, the current study calculated the MNDWI (Xu, 2005) (Eqn (1)) from Landsat-8 image in the early phase of crop growing season to enhance the spectral differences between vegetation, water and dry-bare soil in the fields, and established a decision threshold rule to segment paddy rice and dryland crops (Eqn (2)).

$$\text{MNDWI} = (\rho_{\text{Green}} - \rho_{\text{SWIR2}})/(\rho_{\text{Green}} + \rho_{\text{SWIR2}}) \quad (1)$$

$$\text{MNDWI} = \begin{cases} -0.1 \leq \text{MNDWI} \leq 1, \text{ paddy rice} \\ \text{MNDWI} < -0.1, \text{ dry land crops} \end{cases} \quad (2)$$

where ρ_{Green}, ρ_{SWIR2} represent the Landsat-8 reflectance in the green band (0.53∼0.59 μm) and shortwave infrared band (1.56–1.66 μm), respectively.

A pixel-wise validation was implemented to assess the accuracies of 2014/2016/2020 CDLs (Dong *et al.*, 2016). The current work used a stratified random sampling method to generate ground truth sampling sites across. First, the study region was divided into three zones (paddy rice, dryland crop, non-crop) based on the 2015/2017/2017 CDLs, and randomly settled 600 sampling sites for each zone (Fig. 1(c)). Then, created one region of interest (ROI) for each sampling site; with the high-resolution satellite imagery and Landsat-8 colour composite images as ground truth references, the current work visually interpreted the ground-truth land attribute and compared it with the classified land type on the 2014/2016/2020 CDLs for each ROI. Figures 1(d) and (e) show the ROI examples. Finally, five classification metrics (producer's accuracy, user's accuracy, overall accuracy and Kappa coefficients) were calculated from the confusion matrix to quantify the classification accuracies of 2014/2016/2020 CDLs. The calculation equations of classification metrics refer to Hao *et al.* (2020).

Annual spatio-temporal dynamics of paddy rice and dryland crops

Based on the annual crop layers of the Sanjiang Plain from 2014 to 2020, the current study quantified the changing magnitude and rate of cultivation area for paddy rice and dryland crops at the interannual scale. It also measured the spatial evolution of paddy rice and dryland crops in terms of spatial agglomeration
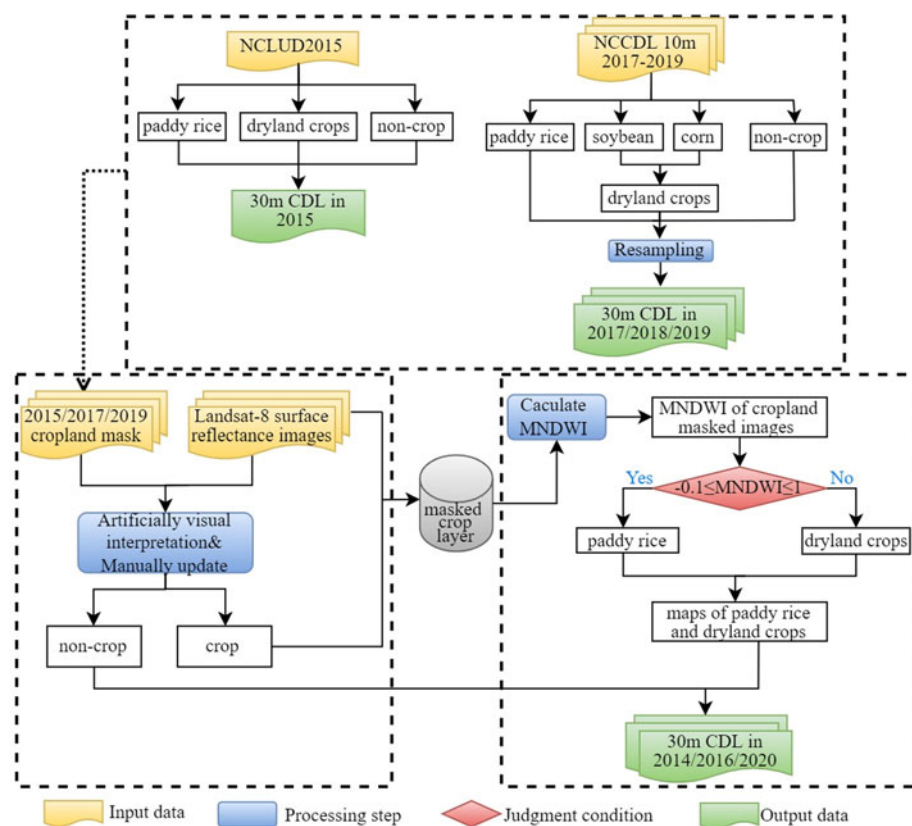
Fig. 2. The conceptual framework of decision tree classification of 30 m annual crop data layers (CDLs) in the Sanjiang plain, during 2014–2020. NCLUD: Northeast China Land Use Data, NCCDL10 m: Northeast China Crop Data Layer.

and directionality by calculating the planted frequencies, changing trend of cultivated area and gravity migration at the pixel scale.

Temporal dynamic analysis

Area variation (Δs) and rate of variation ($\Delta s'$) were used to quantify interannual fluctuations of total planted area for paddy rice and dryland crops. Δs is the total area variation, and $\Delta s'$ is the area variation per unit area for paddy rice or dryland crops.

$$\Delta s = S_b - S_a, \quad \Delta s' = \frac{S_b - S_a}{S_a} \times 100\% \quad (3)$$

where S_a, S_b denote the total planted area of paddy rice (dryland crops) for the two adjacent years.

Spatial dynamic analysis

Frequency statistical analysis

The current work overlaid the annual 30 m CDLs during 2014–2020 at the pixel level, and generated frequency maps of paddy rice and dryland crops over the Sanjiang Plain. The frequency value, ranging from 1 to 7, stands for the number of years planted as paddy rice (dryland crops), and can represent the cropping intensity for the two crop types within the 7 years for each pixel. Then designated the pixels with the 6≤ frequency ≤7, 4≤ frequency <6, and 1≤ frequency <4 as continuous, stable, unstable cultivation, respectively. Note that unstable cultivated fields refer to the fields that might be under crop rotation, fallow or abandoned. Compared with the analysis of annual CDL maps, the frequency statistic maps can show the spatial distribution of paddy

and dryland cropping landscape patterns and its temporal variation in an integrated manner.

Trend analysis

The current study calculated the area fraction percentage within 1 km × 1 km grids for the two crops. Area variation trend (slope) maps of crop planting area were generated at grid scales:

$$slope = \frac{\left[n\sum_{j=1}^n j \times y - \left(\sum_{j=1}^n j\right)\left(\sum_{j=1}^n y\right)\right]}{\left[n \times \sum_{j=1}^n j^2 - \left(\sum_{j=1}^n j\right)^2\right]} \quad (4)$$

where slope is the linear-fitted slope of n years ($n = 7$); y is area fraction for paddy field (or dryland crops) within 1 km × 1 km grids; slope > 0 indicates that crop area shows increasing trend; otherwise, declining trend. The area change trend was further reclassified into five classes based on slope according to the following principles:

$$slope = \begin{cases} slope < mean - 2 \times std, & \text{Significantly decrease} \\ mean - 2 \times std < slope < mean - std, & \text{Decrease} \\ mean - std < slope < mean + std, & \text{No change} \\ mean + std < slope < mean + 2 \times std, & \text{Increase} \\ slope > mean + 2 \times std, & \text{Significantly increase} \end{cases}$$
$$(5)$$

Gravity centre migration model

The gravity centre refers to a spatial mean centre of the area composed of paddy rice and dryland crops field patches. In the current study, the direction and distance of the gravity centre

(X_t, Y_t) at different study nodes are obtained by the gravity centre migration model, in which the direction of gravity deviation indicates the 'high density' of the distribution of paddy rice and dryland crops, and the distance of deviation indicates the equilibrium of migration, thus quantitatively describing the directional characteristics of the spatial evolution of paddy rice and dryland crops:

$$X_t = \frac{\sum_{i=1}^{n} M_{it}X_i}{\sum_{i=1}^{n} M_{it}}, \ Y_t = \frac{\sum_{i=1}^{n} M_{it}Y_i}{\sum_{i=1}^{n} M_{it}} \qquad (6)$$

$$d = \sqrt{(x_{k+m} - x_k)^2 + (y_{k+m} - y_m)^2} \qquad (7)$$

where d is the migration distance between years ($t + 1$ and t, $t =$ 2014–2020); (X_i, Y_i) and M_{it} are the geographical centroid and area for each crop patch, respectively, n is the number of rice (dryland crops) patches.

Results

Remote sensing extraction of paddy rice and dryland crops in 2014, 2016 and 2020

The classification confusion matrix shows that the overall classification accuracies of crop data layers in 2014, 2016 and 2020 exceeded 96%, with the Kappa coefficient ranging from 0.96 to 0.98 (Table 3). MNDWI can effectively distinguish paddy rice from dryland crops, with over 90% accuracy. The average user and producer accuracy for paddy rice is 95% and 90%, respectively; and for dryland crops is 95% and 90%. The classification accuracies for non-crop are greater than 95%. Note that in the current study, satellite imagery from April to June were used to

identify the flooding signal of paddy fields. The availability of imagery during the early rice growing season would affect classification results. For instance, if the date of image acquisition is earlier than the time of field flooding, the spectral signals of rice transplanting cannot be captured; therefore, the identification of paddy rice might fail. In addition, pixels along the boundary between rice fields and dryland crops are affected by the mixed spectrum problem, which reduces the robustness of the MNDWI segment threshold and leads to the classification errors of paddy rice. In Table 3, the omission errors of paddy rice in the confusion matrices are higher than those of other types: 8.85% (2014), 3.25% (2016) and 13.47% (2020).

Figure 3 shows the annual spatial distribution of crop area for the Sanjiang Plain from 2014 to 2020. For 7 years in the Sanjiang Plain, croplands were the main land cover and consist of paddy rice and dryland crops fields, which distributed in the plain areas with low altitude and flat terrain. Paddy rice cultivation was more intensive, and mostly located in water-rich areas, such as the north counties including Fuyuan, Tongjiang, Suibin and Fujin and the south-east region-Hulin County. Note that there were spatial pattern fluctuations of paddy fields in some local areas among years. Especially, paddy rice showed significant expansion in the northeast of Huachuan and the Woken basin. The planting area of paddy rice in the eastern part of Raohe County declined slightly. The dryland crops were mainly located in the north-central counties (Jixian, Jiamusi and Baoqing) and also in the south-western regions (Huanan, Yilan and Boli). Compared to paddy rice, the landscape of dryland crops was more fragmented than paddy rice, and showed circular, striped distributions around the paddy patches. From 2014 to 2020, dryland crops cultivation tended to shrink in Jixian and Muling, and expand in northeastern Fuyuan and the eastern Raohe.

Table 3. Confusion matrix of cropland dataset of the Sanjiang Plain in 2014, 2016 and 2020. Map categories are rows while reference categories are columns. Map categories are rows while reference categories are columns

| Year		Paddy rice	Dryland crops	Other land	Sum	User's accuracy (%)
2014	Paddy rice	32 691	625	131	33 447	91.2
	Dryland crops	3150	48 992	736	52 878	98.1
	Non-crop	26	319	171 868	172 213	99.5
	Sum	35 867	49 936	172 735	258 538	
	Producer's accuracy (%)	97.7	92.7	99.8		Overall accuracy = 98.2%
						Kappa coefficient = 0.96
2016	Paddy rice	24 561	12	338	24 911	96.8
	Dryland crops	644	21 216	503	22 363	99.4
	Non-crop	182	122	156 433	156 737	99.5
	Sum	25 387	21 350	157 274	204 011	
	Producer's accuracy (%)	98.6	94.9	99.8		Overall accuracy = 99.1%
						Kappa coefficient = 0.98
2020	Paddy rice	3063	190	42	3295	92.40
	Dryland crops	468	19 723	583	20 774	94.49
	Non-crop	9	230	67 605	67 844	97.59
	Sum	3540	20 143	68 230	91 913	
	Producer's accuracy (%)	86.5	97.9	95.0		Overall accuracy = 96.8%
						Kappa coefficient = 0.96
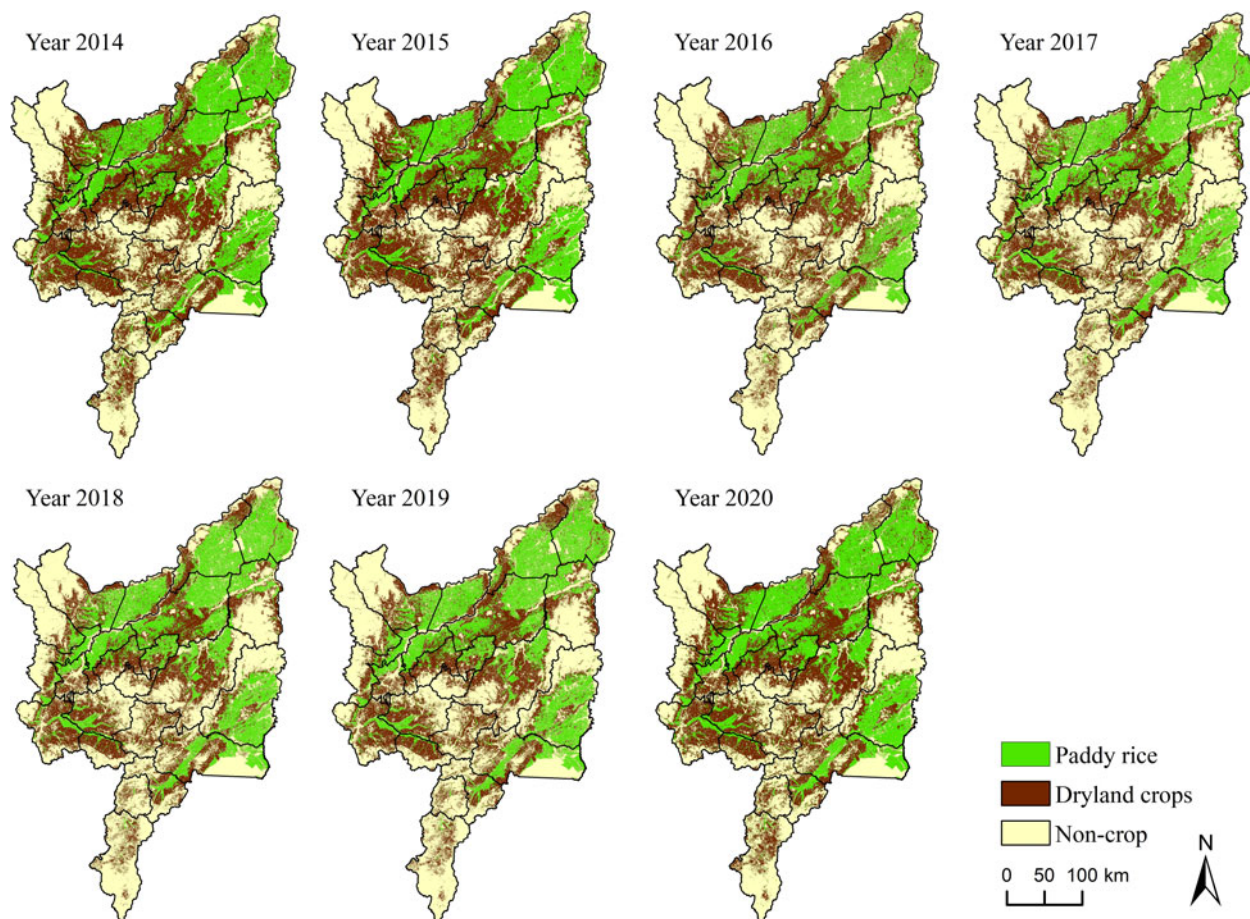
Fig. 3. 30 m annual crop data layers of the Sanjiang Plain in 2014–2020.

Annual temporal characteristics of paddy rice and dryland crops from 2014 to 2020

A comparative analysis of the annual area changes of crop layers during 2014–2020 can accurately demonstrate area variations in paddy rice and dryland crops on the temporal scale (Fig. 4). Cropland was the main land cover in the Sanjiang Plain, accounting for an annual average area percentage of $52 \pm 3.4\%$ ($566 \pm 36.9 \times 10^4 \, \text{hm}^2$). The annual average planting area of dryland crops ($305.3 \pm 29 \times 10^4 \, \text{hm}^2$) was higher than that of paddy rice ($260.9 \pm 14 \times 10^4 \, \text{hm}^2$); the area proportions for paddy rice and dryland crops were 21–25% and 25–32%, respectively (Fig. 4 (b)). The total cropland area reduced from $624.4 \times 10^4 \, \text{hm}^2$ in 2014 to $580 \times 10^4 \, \text{hm}^2$ in 2020, with a decrease of $15.3 \times 10^4 \, \text{hm}^2$, $29.4 \times 10^4 \, \text{hm}^2$ for paddy rice and dryland crops, respectively (Fig. 4(c)). Area variation between 2014–2017 for two croplands were greater than that between 2017–2020; The average absolute area changes in 2014–2017 for paddy rice and dryland crops were $29 \times 10^4 \, \text{hm}^2$, $27 \times 10^4 \, \text{hm}^2$, while in 2017–2020 they were $10 \times 10^4 \, \text{hm}^2$ and $15 \times 10^4 \, \text{hm}^2$, respectively. The unit area change ($\Delta s'$) in paddy rice was −4.5% (2014–2015), −14.1% (2015–2016) and 15.7% (2016–2017), and remained relatively stable (−2.2–5.8%) in other years (Fig. 4(d)). $\Delta s'$ for dryland crops decreased by 10.8% (2015–2016) and 13.2% (2016–2017) and increased slightly after 2017. $\Delta s'$ values were of dryland crops were 2.3% (2017–2018), 3.5% (2018–2019) and 10.6% (2019–2020).

Annual spatial characteristics of paddy rice and dryland crops from 2014 to 2020

Figure 5 shows the statistics of planting frequency for two crops at pixel level. 77.5% of the Sanjiang Plain was once cultivated as cropland for at least one year in 2014–2020 (frequency≥1), with 28.9% and 48.5% for paddy rice and dryland crops, respectively. The landscape pattern of core planting regions of paddy rice was clustered and kept stable over the years. The pixels planted more than 6-year paddy rice accounted for 60% of the total area, which was mainly located in northern counties, such as (Fuyuan, Tongjiang, Suibin and Fujin) (Fig. 5(a)). 24.2% of paddy rice was under 4-year planting frequency, mainly in Huachuan and Raohe. In contrast to paddy rice, the dryland crops cultivation was less stable with fragmented landscape patterns. 48% of the dryland crops have been cultivated for more than 6 years, mainly in the north-central (Fujin, Youyi, Jixian and Baoqing) and southwestern (Yilan, Huanan and Boli) counties (Fig. 5(b)). Compared to paddy rice, the spatial variation was greater in dryland crops with 41.8% planted less than 4 years. One part was scattered in the core area of paddy fields, the other part was located in Jixi and Muling counties with relatively concentrated and spatially coherent patterns.

The current study calculated the trends of area change of two crops at $1 \, \text{km} \times 1 \, \text{km}$ grids within 7 years. For both crops, the regions with an unchanged (Figs 6(a) and (b)) coincided with the areas where cultivation was frequent (Figs 5(a) and (b)). For
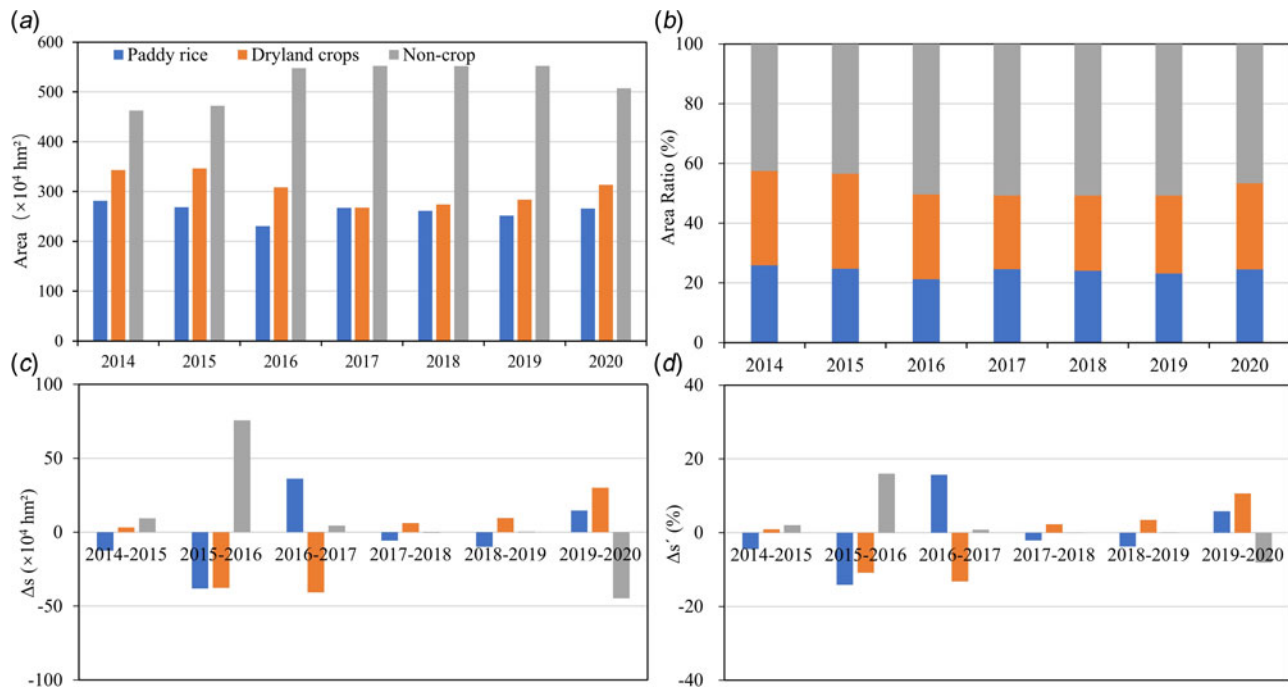
Fig. 4. Statistics of annual area variation for paddy rice and dryland crops in the Sanjiang Plain, 2014–2020: Area (a), Area ratio (b), Area variation (Δs) (c) and rate of variation (Δs′) (d).

paddy rice, the regions with significant increase and increase trends of planted area accounted for 4.2% and 22.3%, respectively; and significant decrease and decrease trends took up to 2.1% and 5.9%, respectively. As for dryland crops, the percentages of significant increase, increase, significant decrease and decrease were 2.5%, 7.0%, 5.7% and 3.5%, respectively. Note that the regions where paddy cultivation was increasing have a

concurrent declining trend in dryland crops cultivation. These regions were mainly located along the water-rich counties, including Huachuan, west Fujin, north Youyi and the intersection of Yilan, Boli and Huanan. Meanwhile, the area with paddy rice cultivation decreasing also corresponded to the area with increasing tendency for dryland crops, with Fuyuan and eastern Raohe as typical regions.
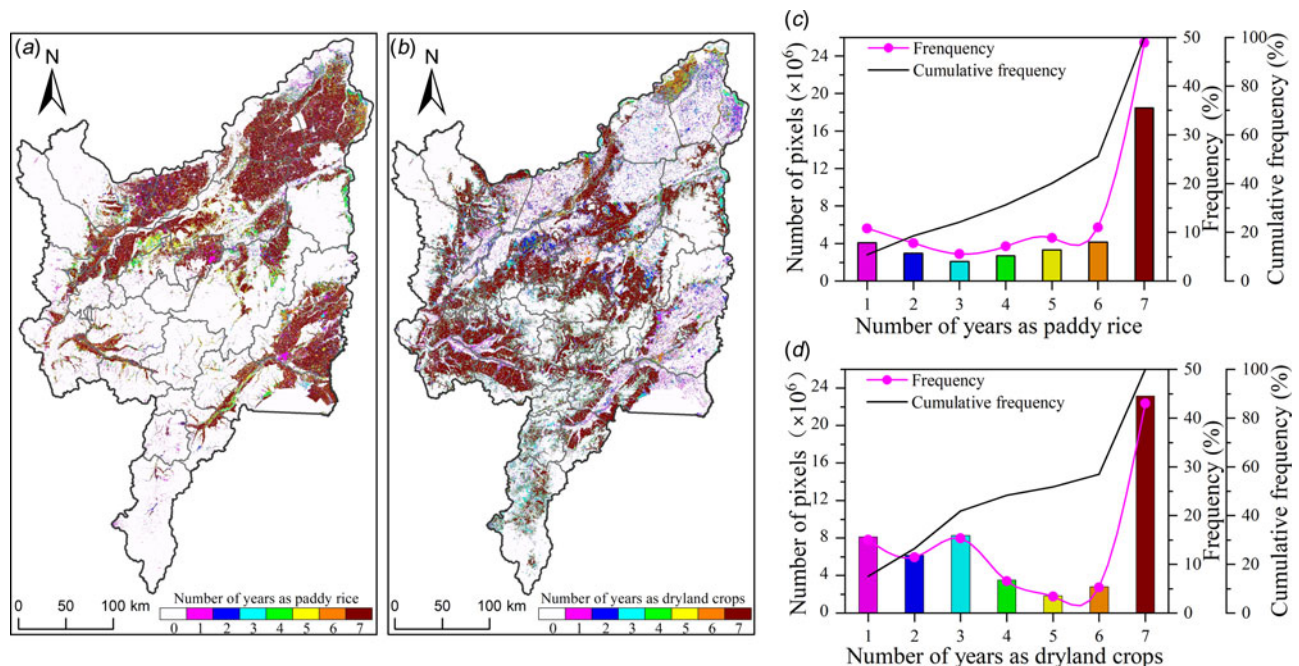

Fig. 5. Frequency statistic maps of paddy rice and dryland crops in the Sanjiang Plain, 2014–2020: frequency maps for paddy rice (a) and dryland crops (b); frequency histograms of paddy rice (c) and dryland crops (d).
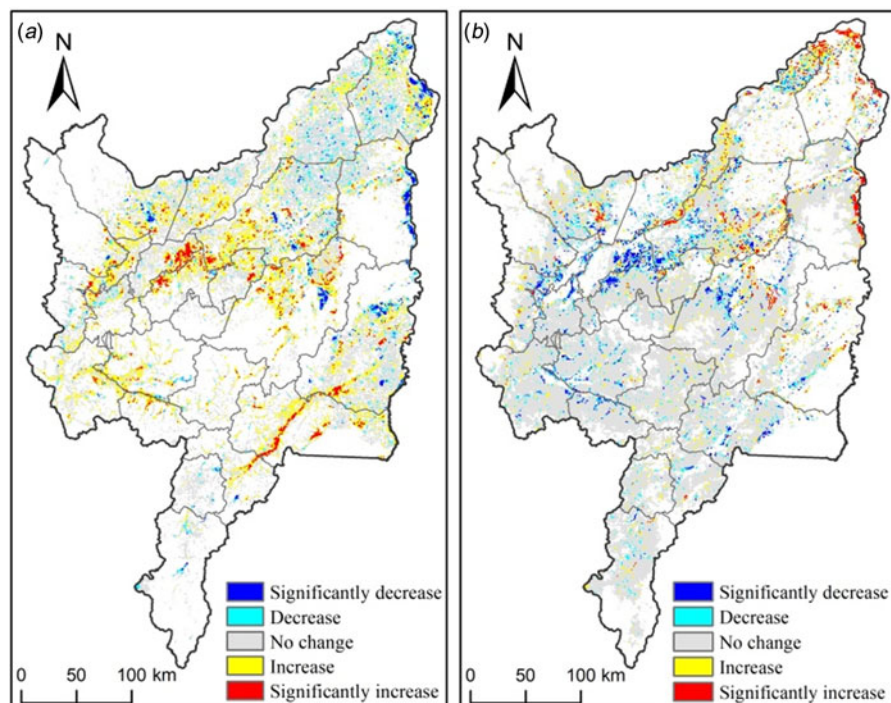
Fig. 6. Slopes of 7-year area percentage within 1 km × 1 km grids for paddy rice (a) and dryland crops (b) in the Sanjiang Plain, 2014–2020.

In 7 years, the centres of gravity for both crops mainly aggregated in the central counties of the Sanjiang Plain (Baoqing, Youyi and Fujin); however, the migration direction and magnitude of the centres of gravity varied from year to year (Fig. 7). Overall, the centre of gravity for paddy rice has shifted 31.8 km to the northeast between 2014 and 2020, while the centres of gravity for dryland crops moved to the opposite by 8.91 km to the southwest. There were significant differences in the migration
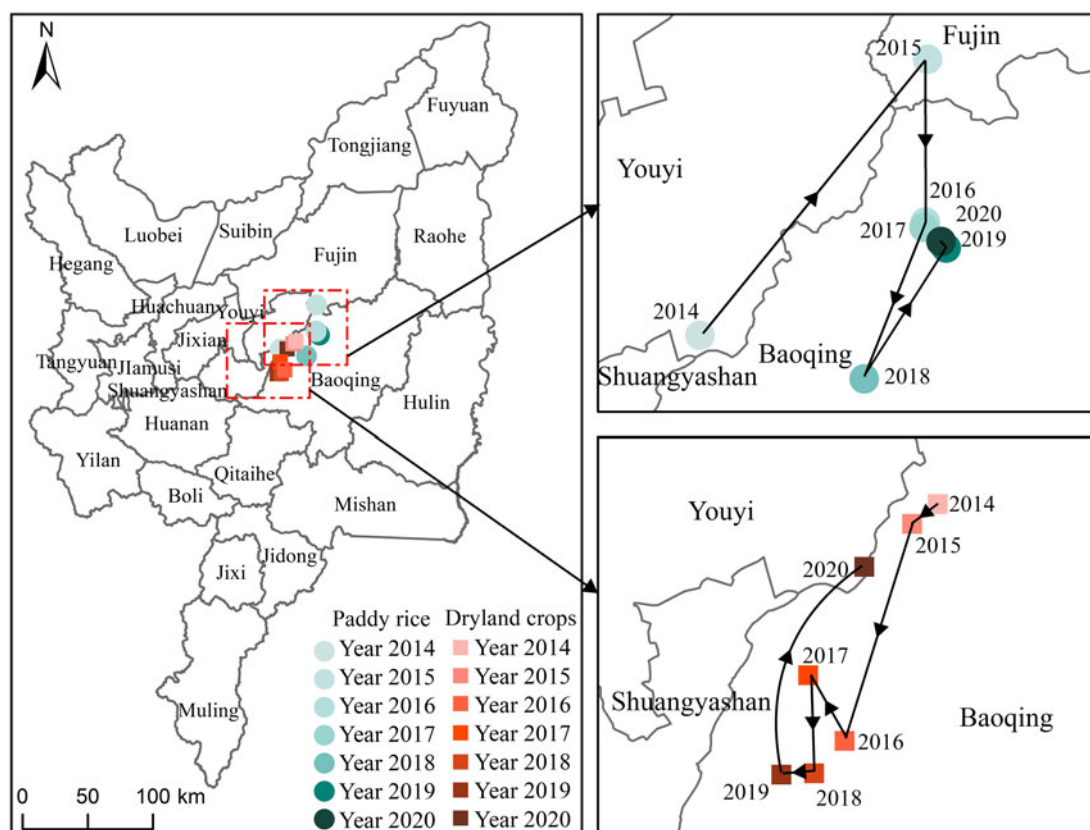

Fig. 7. Trajectory of gravity centres for paddy rice and dryland crops in the Sanjiang Plain, 2014–2020.

trajectories of the two crops. The general trajectory direction of gravity centres of paddy rice was northeast→southwest→ northeast, with a migration speed of 4.54 km/a. In 2014–2015, the migration distance of gravity centres for paddy rice was the largest, around 44.0 km across Youyi to Fujin counties. In 2015–2016, the centre of gravity for paddy rice moved to Baoqing, and then kept stable. The centres of gravity for dryland crops, in general, moved in the southwest→northeast direction, and the average migration speed was 1.27 km/a; Compared to the migration distances in other years (<10 km), the migration distance of dryland crops was greater in 2015–2016 and 2019–2020, 21.0 km toward the southwest and 20.6 km toward the northeast, respectively.

Discussion

Since reclamation in 1954, the Sanjiang Plain has established large state-owned farms and has become an important base for food production in China. Although many studies have artificially interpreted satellite imagery to extract land cover information, and then analysed the spatial pattern evolution of croplands in the Sanjiang Plain, their study period was earlier (1954–2015); In addition, the time interval for quantifying changes in cropland was long. Influenced by a combination of natural and human factors, interannual spatial and temporal variations in cropping patterns of cropland are higher than for non-crop covers (such as built-ups and forests). High-quality, annually updated crop cover dataset can help accurately reflect the spatial distribution of crops, their cultivation structure and intra-annual dynamics. Meanwhile, it can optimize and improve the parameter inputs of modelling crop growth, irrigation, terrestrial ecosystem and improve model prediction accuracies. The visual interpretation method artificially digitizes cropland boundaries from false-colour composite satellite images based on differences in hue, shape, and texture between paddy fields and dryland crops. This method is laborious and its cost of generating annual crop data layers is high. Therefore, the frequency of updating the land cover dataset based on this method is at intervals of 5 years or more. Recent studies have proposed a single phenology-phase mapping algorithm for paddy rice in the Sanjiang Plain based on the relationship between Enhanced Vegetation Index (EVI) and Land Surface Water Index (LSWI) during the transplanting period of rice seedlings. Compared to the visual interpretation approach, these automatic computer recognition algorithms are simpler with less labour and time costs, and higher classification accuracy of paddy rice in the Sanjiang Plain. The users' and producers' accuracies were about 90–97% and 91–94%, respectively (Dong et al., 2015; Qin et al., 2015; Jin et al., 2016). To investigate the recent spatial and temporal changes of cropland in the Sanjiang Plain, the current study collected the cropland datasets of 2015, 2017 and 2019 and updated the cropland boundaries in 2014, 2016 and 2020 from the cropland data of 2015, 2017 and 2019 using false-colour composite satellite imagery; Then, the paddy fields were derived from cropland by setting the thresholds for segmentation of MNDWI in the early cropping season, and built the annual crop layer datasets from 2014 to 2020, whose accuracy (90–95%) is comparable to the accuracy of the previous cropland datasets. Therefore, the current study improves the classification efficiency of croplands while ensuring the classification accuracy of paddy rice and dryland crops.

The early land cover changes of the Sanjiang Plain and the associated environmental effects have received widespread attention, which mainly focused on 1954–2015 (Zhou et al., 2009; Song et al., 2014; Yan and Zhang, 2019). Studies show that since 1949, with the increase in food demand and population growth, the Sanjiang Plain has experienced the reclamation of natural vegetation (wetlands and grasslands) to cropland and the large-scale conversion of dryland crops to paddy fields, which is called the rapid agricultural development period (Wang et al., 2011); Until the beginning of the 21st century, the ecological environment was severely threatened by the rapid expansion of cultivated land. Wetland protection policies such as wetland restoration, have slowed the expansion of cropland to some degree (Wang et al., 2006; Liu et al., 2015). A highly intensive pattern of agricultural land use emerged in the 2005–2015 period. For instance, paddy rice was large-scale mechanized cultivated, while the landscape patterns of dryland crops were fragmented. The cropland unsuitable for cultivation was restored as wetland (grassland or forest), and wetlands showed a marked decline in reclamation rates (Wang et al., 2019; Xiang et al., 2020). To follow up on previous studies, it was found that despite the cultivation structure and spatial pattern of croplands were relatively stable during 2014–2020, the cultivated area of paddy rice and dryland crops showed a slight overall declining trend with positive and negative interannual fluctuations. Natural environmental and socioeconomic factors are the main drivers causing the changes in cropping patterns in the Sanjiang Plain. Natural factors such as climate, topography and hydrologic conditions directly determine the overall spatial suitability of regional crop planting, with little short-term variation; Unlike natural factors, socioeconomic backgrounds, including market demand, economic efficiency, agricultural macro-control and resource and environmental protection policies, are highly volatile and have rapid and significant effects on short-term changes in agricultural cropping patterns (Chen et al., 2022), and are the main factors contributing to the interannual variation in cropping patterns of two croplands in the current study. Under market economy, farmers' production decisions are driven by market efficiency (i.e., planting production costs and returns are related), which in turn determine the agricultural planting structure. The purchase price of rice in Heilongjiang Province was reduced from RMB 3.0/kg in 2017 to RMB 2.6/kg in 2018, and this price remained until 2021. Meanwhile, the cost of agricultural inputs has been considerable, the cost of planting and harvesting rice has increased by years, and the land rent for rice cultivation has also increased. According to the law of diminishing land returns, paddy rice cultivation with less economic benefits is reduced, and some rice planting areas are replaced by dryland crops with better economic returns. Strengthened by the policy guidance in recent years, Heilongjiang Province optimized the regional agricultural cultivation structure and proposed to appropriately reduce the cultivation of paddy rice in the areas of the Sanjiang Plain with inferior and inefficient soils and in the areas with excessive groundwater exploitation, and advocated corn-soybean rotation, and appropriately expanded soybean cultivation. The interannual variation in the gravity centre of paddy rice and dryland crops in the Sanjiang Plain is mainly driven by human-led land use behaviour. From 2014 to 2015, the gravity centre of paddy rice and dryland crops migrated to the northeast, mainly due to the expansion of paddy rice in Fuyuan and Tongjiang in the north during this period. During the period 2015–2018, the gravity centre of paddy rice moved southwards, mainly because some counties in the southwestern of the Sanjiang Plain (e.g. Huachuan) were affected by the low efficiency of paddy rice and government

regulation, and vigorously promoted the 'dryland crops convert to paddy rice' in order to adjust the cropland cultivation pattern. In addition, benefiting from the vigorous development of water conservancy projects during this period, the increase in the cultivation of paddy fields in the southern Muling and Umken river basins contributed to the southward migration of the gravity centre of paddy field cultivation. Since 2018, in order to curb groundwater over-exploitation in the Sanjiang Plain to ensure the sustainable development of agriculture (Li *et al.*, 2021), Heilongjiang Province has focused on the pilot work of fallowing paddy fields in the southern part of the Sanjiang Plain (Chong *et al.*, 2020), of which the fallowed paddy fields in Hulin and Baoqing have contributed to the northward migration of the gravity centre of paddy field cultivation. The gravity centre of dryland crops showed a continuous southward migration from 2014 to 2019, which was also influenced by the policy of vigorously promoting the 'dryland crops convert to paddy rice' in some counties in the southwestern part of the Sanjiang Plain, as mentioned above, In addition, the economic development of the southern of Heilongjiang Province (Mudanjiang) during this period was accompanied by the expansion of dryland fields in accordance with the principle of 'balance of occupation', which also led to a significant migration in the centre of gravity of dryland fields southwards. In 2019–2020, the centre of gravity of the dryland crops moved towards the northeast, due to the impact of the national policy of subsidizing dryland crops and the 'paddy rice to dryland crops' in the eastern of Sanjiang plain (Hulin city).

The current study relied on available land cover products and satellite images during the early cropping season to create 3-period 30 m crop layers through a combination of visual interpretation and threshold segmentation. Although the classification strategy in the current study can separate paddy rice from dryland crops quickly and with satisfactory classification accuracy, classification efficiency is limited by the effort required to update cropland boundaries; secondly, the seven crop datasets were derived from three different classification strategies, leading to inconsistent classification system errors across the datasets, reducing their comparability and increasing uncertainties in interannual spatiotemporal dynamic analysis of two croplands. In the future, under the background to optimize regional crop planting patterns, frequent crop rotations (e.g., rice to soybean and corn-soybean rotation) will urgently require agricultural land datasets covering more crop types. With the support of cloud computing platform for remote sensing big data (e.g., GEE, PIE- Engine) and very high-resolution satellite data, a standardized and operational production and assessment systems for regional crop datasets need future efforts.

Conclusions

The current study established the annual 30 m crop datasets for 2014–2020. It explained the spatial distribution characteristics of crop cultivation of the Sanjiang Plain in recent years, and investigated spatio-temporal dynamic process of the regional crop cultivation structure. The classification strategy proposed in the study can effectively constructed high-quality spatial datasets for croplands. Even though the total planted area of both crop declined slightly from 2014 to 2020, it shows obvious interannual variations in total area, cropping frequency, area change trend and trajectories of centres of gravity along continuous years. The current study theoretically highlight key aspects that have been neglected in studies of monitoring land cover change monitoring,

that is, quantifying the annual process of land cover change is more important than describing its initial and final status. In terms of practical applications, these results also provide fundamental scientific insights for optimal regulation of regional agricultural resources, sustainable use of cropland and ensuring food security.

Author contributions. J. C. and Z. ZY. conceived and designed the study. Z. ZY., C. G. and L. XT. contributed to the remote sensing data collection and classification. J. C. and Z. ZY. drafted the manuscript, revised the manuscript and approved the final version. L. XM. and C. HY. contributed to the revision of the final version. All authors read and approved the final manuscript.

Conflict of interest. The authors declare there are no conflicts of interest.

Ethical standards. Not applicable.

References

Amani M, Kakooei M, Moghimi A, Ghorbanian A, Ranjgar B, Mahdavi S, Davidson A, Fisette T, Rollin P and Brisco B (2020) Application of Google Earth Engine cloud computing platform, sentinel imagery, and neural networks for crop mapping in Canada. *Remote Sensing* **12**, 3561.

Blickensdörfer L, Schwieder M, Pflugmacher D, Nendel C, Erasmi S and Hostert P (2022) Mapping of crop types and crop sequences with combined time series of Sentinel-1, Sentinel-2 and Landsat 8 data for Germany. *Remote Sensing of Environment* **269**, 112831.

Boryan C, Yang ZW, Mueller R and Craig M (2011) Monitoring US agriculture: the US department of agriculture, national agricultural statistics service, cropland data layer program. *Geocarto International* **26**, 341–358.

Cai Z, Li SS, Du GM and Xue RH (2021) Linking smallholder farmers to the heilongjiang province crop rotation project: assessing the impact on production and well-being. *Sustainability* **14**, 38.

Chen YL, Lu DS, Moran E, Batistella M, Dutra LV, Sanches IDA, Da Silva RFB, Huang JF, Luiz AJB and MaF DO (2018) Mapping croplands, cropping patterns, and crop types using MODIS time-series data. *International Journal of Applied Earth Observation and Geoinformation* **69**, 133–147.

Chen H, Meng F, Yu ZN and Tan YZ (2022) Spatial–temporal characteristics and influencing factors of farmland expansion in different agricultural regions of Heilongjiang Province, China. *Land Use Policy* **115**, 106007.

Chong L, Liu HJ, Qiang F, Guan HX, Qiang Y, Zhang XL and Kong FC (2020) Mapping the fallowed area of paddy fields on Sanjiang Plain of Northeast China to assist water security assessments. *Journal of Integrative Agriculture* **19**, 1885–1896.

Defourny P, Bontemps S, Bellemans N, Cara C, Dedieu G, Guzzonato E, Hagolle O, Inglada J, Nicola L, Rabaute T, Savinaud M, Udroiu C, Valero S, Bégué A, Dejoux J-F, El Harti A, Ezzahar J, Kussul N, Labbassi K, Lebourgeois V, Miao Z, Newby T, Nyamugama A, Salh N, Shelestov A, Simonneaux V, Traore PS, Traore SS and Koetz B (2019) Near real-time agriculture monitoring at national scale at parcel resolution: performance assessment of the Sen2-Agri automated system in various cropping systems around the world. *Remote Sensing of Environment* **221**, 551–568.

Dong JW, Xiao XM, Kou WL, Qin YW, Zhang GL, Li L, Jin C, Zhou YT, Wang J and Biradar C (2015) Tracking the dynamics of paddy rice planting area in 1986–2010 through time series Landsat images and phenology-based algorithms. *Remote Sensing of Environment* **160**, 99–113.

Dong JW, Xiao XM, Menarguez MA, Zhang GL, Qin YW, Thau D, Biradar C and Moore Iii B (2016) Mapping paddy rice planting area in northeastern Asia with Landsat 8 images, phenology-based algorithm and Google Earth Engine. *Remote Sensing of Environment* **185**, 142–154.

Du GM, Li Y, Yu FR, Zhang SW and Yang FH (2012) Change characteristics analysis of farmland in Northern Sanjiang Plain in 2000–2009 based on remote sensing. *Transactions of the Chinese Society of Agricultural Engineering* 28, 225–229.

Fan X, Zhang W, Chen WW and Chen B (2020) Land–water–energy nexus in agricultural management for greenhouse gas mitigation. *Applied Energy* 265, 114796.

Fisette T, Rollin P, Aly Z, Campbell L, Daneshfar B, Filyer P, Smith A, Davidson A, Shang J and Jarvis I (2013) AAFC annual crop inventory. *Second International Conference on Agro-Geoinformatics*, pp. 270–274.

Hao PY, Di LP, Zhang C and Guo LY (2020) Transfer learning for crop classification with cropland data layer data (CDL) as training samples. *Science of The Total Environment* 733, 138869.

Hu Q, Yin H, Friedl MA, You LZ, Li ZL, Tang HJ and Wu WB (2021) Integrating coarse-resolution images and agricultural statistics to generate sub-pixel crop type maps and reconciled area estimates. *Remote Sensing of Environment* 258, 112365.

Huang N, Liu D and Wang ZM (2009) Study on mutual transformation characteristics between paddy field and dry land in Sanjiang Plain from 1986 to 2005. *Resources Science* 2, 324–329.

Jin C, Xiao XM, Dong JW, Qin YW and Wang ZM (2016) Mapping paddy rice distribution using multi-temporal Landsat imagery in the Sanjiang Plain, Northeast China. *Frontiers of earth science* 10, 49–62.

Li D, Tian PP, Luo YF, Dong B, Cui YL and Khan S (2021) Importance of stopping groundwater irrigation for balancing agriculture and wetland ecosystem. *Ecological Indicators* 127, 107747.

Lin SY (2023) Restoring the state back to food regime theory: china's agribusiness and the global soybean commodity chain. *Journal of Contemporary Asia* 53, 288–310.

Liu JP, Sheng LX, Lu XG and Liu Y (2015) A dynamic change map of marshes in the Small Sanjiang Plain, Heilongjiang, China, from 1955 to 2005. *Wetlands Ecology and Management* 23, 419–437.

Luo YC, Zhang Z, Zhang LL, Han JC, Cao J and Zhang J (2022) Developing high-resolution crop maps for major crops in the European Union based on transductive transfer learning and limited ground data. *Remote Sensing* 14, 1809.

Mao DH, Wang ZM, Wu JG, Wu BF, Zeng Y, Song KS, Yi KP and Luo L (2018) China's wetlands loss to urban expansion. *Land Degradation & Development* 29, 2644–2657.

Mao DH, He XY, Wang ZM, Tian YL, Xiang HX, Yu H, Man WD, Jia MM, Ren CY and Zheng HF (2019) Diverse policies leading to contrasting impacts on land cover and ecosystem services in Northeast China. *Journal of Cleaner Production* 240, 117961.

Pan T, Zhang C, Kuang WH, De Maeyer P, Kurban A, Hamdi R and Du GM (2018) Time tracking of different cropping patterns using Landsat images under different agricultural systems during 1990–2050 in cold China. *Remote Sensing* 10, 2011.

Pan T, Zhang C, Kuang WH, Luo GP, Du GM and Yin ZR (2020) Large-scale rain-fed to paddy farmland conversion modified land-surface thermal properties in Cold China. *Science of The Total Environment* 722, 137917.

Pan T, Zhang C, Kuang WH, Luo GP, Du GM, Demaeyer P and Yin ZR (2021) A large-scale shift of cropland structure profoundly affects grain production in the cold region of China. *Journal of Cleaner Production* 307, 127300.

Qin YW, Xiao XM, Dong JW, Zhou YT, Zhu Z, Zhang GL, Du GM, Jin C, Kou WL and Wang J (2015) Mapping paddy rice planting area in cold temperate climate region through analysis of time series Landsat 8 (OLI), Landsat 7 (ETM+) and MODIS imagery. *ISPRS Journal of Photogrammetry and Remote Sensing* 105, 220–233.

Shi SX, Chang Y, Wang GD, Li Z, Hu YM, Liu M, Li YH, Li BL, Zong M and Huang WT (2020) Planning for the wetland restoration potential based on the viability of the seed bank and the land-use change trajectory in the Sanjiang Plain of China. *Science of The Total Environment* 733, 139208.

Song KS, Liu DW, Wang ZM, Zhang B, Jin C, Li F and Liu HJ (2008) Land use change in Sanjiang Plain and its driving forces analysis since 1954. *Acta Geographica Sinica* 63, 93–104.

Song K, Wang Z, Du J, Liu L, Zeng L and Ren C (2014) Wetland degradation: its driving forces and environmental impacts in the Sanjiang Plain, China. *Environmental Management* 54, 255–271.

Song G, Yang XX, Gao J and University N (2017) Study on the distribution patterns and characteristics of paddy cropland in the typical area of Sanjiang Plain. *China Land Sciences* 31, 61–68.

Song XP, Huang WL, Hansen MC and Potapov P (2021) An evaluation of Landsat, Sentinel-2, Sentinel-1 and MODIS data for crop type mapping. *Science of Remote Sensing* 3, 100018.

Wang ZM, Zhang B, Zhang SQ, Li XY, Liu DW, Song KS, Li JP, Li F and Duan HT (2006) Changes of land use and of ecosystem service values in Sanjiang Plain, Northeast China. *Environmental monitoring and assessment* 112, 69–91.

Wang ZM, Song KS, Liu DW, Zhang B, Zhang SQ, Li F, Ren CY, Jin C, Yang T and Zhang CH (2009) Process of land conversion from marsh into cropland in the Sanjiang Plain during 1954–2005. *Wetland Science* 7, 208–217.

Wang ZM, Song KS, Ma WH, Ren CY, Zhang B, Liu DW, Chen JM and Song CC (2011) Loss and fragmentation of marshes in the Sanjiang Plain, Northeast China, 1954–2005. *Wetlands* 31, 945–954.

Wang GD, Jiang M, Wang M and Xue ZS (2019) Natural revegetation during restoration of wetlands in the Sanjiang Plain, Northeastern China. *Ecological Engineering* 132, 49–55.

Wardlow BD, Egbert SL and Kastens JH (2007) Analysis of time-series MODIS 250 m vegetation index data for crop classification in the US Central Great Plains. *Remote Sensing of Environment* 108, 290–310.

Xiang HX, Wang ZM, Mao DH, Zhang J, Xi YB, Du BJ and Zhang B (2020) What did China's National Wetland Conservation Program Achieve? Observations of changes in land cover and ecosystem services in the Sanjiang Plain. *Journal of Environmental Management* 267, 110623.

Xie J, Sun YR, Liu X, Ding Z and Lu M (2021) Human activities introduced degenerations of Wetlands (1975–2013) across the sanjiang plain north of the Wandashan Mountain, China. *Land* 10, 1361.

Xu HQ (2005) A study on information extraction of water body with the modified normalized difference water index (MNDWI). *Journal of Remote Sensing* 9, 585–595.

Yan FQ and Zhang SW (2019) Ecosystem service decline in response to wetland loss in the Sanjiang Plain, Northeast China. *Ecological Engineering* 130, 117–121.

Yan FQ, Zhang SW, Kuang WH, Du GM, Chen J, Liu XT, Yu LX and Yang CB (2016a) Comparison of cultivated landscape changes under different management modes: a case study in Sanjiang Plain. *Sustainability* 8, 1071.

Yan FQ, Zhang SW, Liu XT, Chen D, Chen J, Bu K, Yang JC and Chang LP (2016b) The effects of spatiotemporal changes in land degradation on ecosystem services values in Sanjiang Plain, China. *Remote Sensing* 8, 917.

Yin LK, You NS, Zhang GL, Huang JX and Dong JW (2020) Optimizing feature selection of individual crop types for improved crop mapping. *Remote Sensing* 12, 162.

You NS, Dong JW, Huang JX, Du GM, Zhang GL, He YL, Yang T, Di YY and Xiao XM (2021) The 10-m crop type maps in northeast China during 2017–2019. *Scientific Data* 8, 1–11.

Zhang M, Wu BF, Zeng HW, He GJ, Liu C, Tao SQ, Zhang Q, Nabil M, Tian FY and Bofana J (2021) GCI30: a global dataset of 30 m cropping intensity using multisource remote sensing imagery. *Earth System Science Data* 13, 4799–4817.

Zhang LY, Wang ZL ESX, Du GM and Chen ZS (2022) Analysis of climatic basis for the change of cultivated land area in Sanjiang Plain of China. *Frontiers in Earth Science* 10, 862141.

Zhou DM, Gong HL, Wang YY, Khan S and Zhao KY (2009) Driving forces for the marsh wetland degradation in the Honghe National nature reserve in Sanjiang Plain, Northeast China. *Environmental Modeling & Assessment* 14, 101–111.